VFAST Transactions on Software Engineering
https://vfast.org/journals/index.php/VTSE@ 2023, ISSN(e): 2309-3978, ISSN(p): 2411-6246
Volume 11, Number 4, October-December 2023 *pp:80-92*

Enhancing Breast Cancer Detection through Thermal Imaging and Customized 2D CNN Classifiers

Saif Ur Rehman Khan [1*], **Asif Raza** [2], **Muhammad Tanveer Meeran** [3], **Umair Bilhaj** [4]

[1]School of Computer and Engineering, Central South University, Changsha, China; [2]Department of Computer Science, Bahauddin Zakariya University, Multan, Pakistan; [3]Department of Computer Science and information technology, University Malaysia terengannu; [3] Department of Computer Science, Institute of Southern Punjab Multan

Keywords:
Thermography, Breast Cancer, CNN, SVM, KNN.

Journal Info:
Submitted:
October 27, 2023
Accepted:
December 25, 2023
Published:
December 31, 2023

Abstract

Breast cancer is one of the most prevalent and life-threatening forms of cancer due to its aggressive nature and high mortality rates. Early detection significantly improves a patient's chances of survival. Currently, mammography is the preferred diagnostic method, but it has drawbacks such as radiation exposure and high costs. In response to these challenges, thermography has become a less invasive and cost-effective alternative, gaining popularity. We aim to develop a cutting-edge model for breast cancer detection based on thermal imaging. The initial phase involves creating a customized machine-learning (ML) model built on convolutional neural networks (CNN). Subsequently, this model undergoes training using a diverse dataset of thermal images depicting breast abnormalities, enabling it to identify breast cancer effectively. This innovative approach promises to revolutionize breast cancer diagnosis and offers a safer and more accessible alternative to traditional methods. In our recent study, we leveraged thermal image processing techniques to forecast breast cancer precisely based on its external manifestations, particularly in cases where multiple factors are interconnected. This research employed various image classification methods to categorize breast cancer effectively. Our comprehensive approach encompassed segmentation, texture-based feature extraction from thermal images, and subsequent image classification, leading to the successful detection of malignant images. Our study harnessed the power of machine learning to create a tailored classifier, merging key components from GoogleNet, including the utilization of 2D CNNs and activation functions, with the ResNet architecture. This hybrid approach incorporated batch normalization layers following each convolutional layer and employed max-pooling to enhance classification accuracy. Next, we used a sample dataset of carefully selected images from DMR-IR to train our proposed model. The outcomes of this training demonstrated significant improvement over existing methods, with our suggested 2D CNN classifiers achieving an impressive classification rate of 95%, surpassing both the SVM and current CNN models, which achieved rates of 91% and 71%, respectively.

***Correspondence author email address:** saifurrehman.khan@csu.edu.cn
DOI: 10.21015/vtse.v11i4.1684

1 Introduction

Cancer originates [1] within the cells that make up our body's tissues. While the human body comprises various types of tissues, breast tissue is notably susceptible to this condition. For a person to thrive, the body must continually generate and divide new cells. This process is essential to replace aging cells that naturally die off over time. However, there are instances when this cellular renewal process goes awry. In these situations, old cells may proliferate and inhibit the growth of new ones, accumulating unnecessary excess cells. This abnormal cell growth ultimately leads to a lump, tumor, or change. Breast tissue inflammation is often an early sign of breast cancer, a hazardous form of malignancy.

Breast cancer has tragically been the leading cause of mortality among women for several decades. Given its profound impact, governments worldwide, particularly in developed nations, have dedicated significant resources to detecting and treating this disease. In the context of breast cancer, a sentinel lymph node is one directly linked to the cancer through lymphatic tissue, presenting a potential site for cancer metastasis. Extensive research has been undertaken in breast cancer diagnosis and classification. research indicate that channel our efforts toward developing an adaptive system capable of accurately identifying and classifying breast cancer [2].

According to reports, breast cancer accounts for 22.9 percent of all invasive malignancies in women. Various techniques are employed for early identification and diagnosis. Early detection of breast cancer is vital and can be achieved through screening, wherein a healthcare professional conducts a physical examination to detect any tumors. Additionally, there are alternative screening methods, such as thermal imaging and other imaging techniques. Early detection is crucial in managing the disease. Mammography stands out as the most widely used method for detecting breast cancer in its early stages, owing to its ease of use, affordability, and effectiveness. However, it's essential to consider its limitations before undergoing the procedure. These drawbacks include exposure to radiation and the potential for discomfort during the process. Furthermore, mammography is reported to have a sensitivity ranging from 70% to 90% and a false-negative rate of 10% to 30% [3]. It is worth noting that mammography may miss more than 25% of all malignancies [4–10], particularly in cases where the breasts are too large and complex to distinguish from one another. Therefore, while mammography is a valuable tool, it may only be infallible in some situations.

According to a recent study conducted by a team of researchers [4], thermal imaging can serve as a valuable primary diagnostic tool in certain situations and complement traditional mammography. The study [11] investigated the potential of ML algorithms for early breast cancer detection. Interestingly, none of the studies included in our research considered the incorporation of specific clinical and personal risk factors for breast cancer, even though these factors are well-established in the field.

The Internet of Things (IoT) has rapidly gained prominence across various commercial and educational sectors, profoundly impacting healthcare. The IoT revolution reshapes current healthcare practices by converging technological, economic, and social perspectives. An example of this transformation is monitoring body temperature, a vital health indicator. Infrared thermography (IRT), in contrast to conventional medical thermometers, offers a non-invasive, contactless, and passive approach to measuring and monitoring body temperature. Furthermore, IRT can remotely assess surface body heat.

Beyond temperature monitoring, IRT has demonstrated its efficacy in diagnosing a range of medical conditions, including cardiovascular issues, diabetic neuropathy, and breast cancer, among others. Over the past few decades [12–18], it has found applications in diverse domains such as gynecology, dermatology, cardiology, maternal physiology, and neuroimaging. The recent advancements in infrared camera technology, data collection, and processing methods have enabled the production of real-time, high-resolution thermographic images. However, in recent years, the Internet of Things (IoT) has emerged as a groundbreaking technological paradigm, driving researchers,

healthcare professionals, and doctors to introduce innovative solutions across various environments, particularly in medical and healthcare services. This progress has been facilitated by intelligent sensors, interconnected computer networks, and remote servers, among other vital components [19–22].

This paper introduces an innovative IoT-enabled medical system that integrates IoT technology with advanced infrared thermography techniques. This integration empowers the system to offer real-time, remote diagnosis and detection capabilities for various medical issues. This system can swiftly identify, diagnose, and promptly notify users of irregularities or health concerns. Main contribution of this study as follow:

- Developed a customized machine learning model based on 2D CNN for breast cancer detection using thermal imaging. Created a fusion model inspired by GoogleNet and ResNet structures, enhancing classification accuracy.
- Utilized a sample dataset of thermal images from the DMR-IR database for training and evaluation. Achieved a classification rate of 95%, outperforming existing SVM and CNN methods.
- Highlighted the potential of thermography as a cost-effective and less invasive breast cancer detection technique. Promoted further research and attention to thermography in breast cancer diagnosis.

2 Related Work

One of the leading causes of death for women globally is breast cancer; for the classification of breast thermograms, cutting-edge engineering and artificial intelligence technologies have been employed. For professionals, thermal imaging categorization saves time. Although there are many studies on the classification of breast images, few review papers offer a thorough rundown of methods, feature extraction, classification parameters, and results. In addition to alternative classifiers, the research emphasizes the CNN approach for breast image categorization [23].

The integration of many ML techniques has contributed to the success of ML approaches and tools for treating patients with breast cancer. One central area for improvement with the existing deep learning model-based ML classifiers is their computational complexity. The goal of this work is to create a DNN model that is lightweight for faster building. Furthermore, a DNN-based model that uses a cancer image classifier needs much training data. In addition to breast thermogram datasets, generalized image classification approaches, feature extraction, noise reduction strategies, performance measurement criteria, and the most recent research, this study offers a thorough overview of breast cancer image classification methodologies. Patients may have to wait longer than expected since there are insufficient specialists. Immediate disease feedback from an ML-based diagnostic system can improve patient treatment outcomes [19].

In study [27], they implemented four distinct neural network models: Back Propagation Algorithm (BPA), Radial Basis Function Networks (RBFN), Learning vector Quantization (LVQ), and Competitive Learning Network (CL). They found that the LVQ is the most effective classifier for detecting breast cancer after doing research [19]. Three modules are used in this paper's hybrid system for identifying breast cancer tumors: fuzzy features for feature extraction, hybrid bees algorithm for back-propagation training, and a multi-layer perceptron neural network for classifier. High accuracy was attained by this model [20]. After testing it on four datasets, they also presented a partially connected neural network technique comparable to fully secured neural networks.

The most advanced technique available for accomplishing this goal is mammography-based breast cancer screening. It cannot, however, be used to treat patients with tumors smaller than 2 mm or dense breasts. Four steps make up the thermographic breast cancer detection method: image pre-processing using versatile histogram equalization and beaver hat transform, K-mean clustering and binary masking for ROI segmentation, signature boundary feature extraction, and classification using the ELM and MLP. When the suggested approach was tested using the DMR-IR public dataset, the ELM-based model outperformed the MLP-based

model regarding outcomes [24]. With a small dataset, they used a hybrid approach [25] that included a feed-forward neural network and a gradient descent training algorithm to achieve excellent classification accuracy and a low false-positive ratio.

Author [26] suggested utilizing a Fast Fuzzy C-mean technique enhanced with Neutrosophic submodules for the automatic segmentation and categorization of normal and abnormal breasts. An SVM classifier was used to determine if an image was normal or aberrant. Nevertheless, generalizing the findings is hindered by the study's small sample size, which consisted of 29 healthy participants and 34 cancer patients.

The authors [27] looked at seven deep CNN models to classify breast thermograms. The learning rate was set at 1e-4, and 141 thermal images of healthy individuals and 32 thermal images of breast cancer patients were used, with 70% of the dataset used for training and 30% for verification. A total of 5 epochs were employed. Sensitivity, specificity, accuracy, and area under the ROC curve were used to gauge performance. To show how valuable an SVM classifier is for early-stage breast cancer diagnosis, the authors [28] merged it with Inception V3. They adjusted the model using a particular learning rate of 1e-4 utilizing a database that included normal and aberrant thermal images. Throughout 15 epochs, training and testing used 80% and 20% of the data, respectively. The study demonstrated Inception V3's aptitude for handling a variety of input formats and its capacity for precise classification.

The study [30] concentrated on building an extensive database and analyzing 180 people with breast cancer. For point-wise classification and segmentation modeling techniques, the authors used a variety of CNN architectures and improved their models using the Adam optimization technique with varying learning rates. Of all the networks examined, V-net showed itself to be the most accurate.

In this series of papers, the authors explored the use of advanced deep-learning [31–34] techniques for breast cancer detection and thermal image analysis. They employed deep CNNs, ML classifiers , ensembles techniques and U-net to address different aspects of the problem.

3 Method and Materials

This section introduces a modified 2D-CNN model designed to improve breast cancer detection significantly. This advanced technology enables swift differentiation between malignant and benign tumors, offering several key advantages. One notable benefit is its ability to automatically extract essential features without extensive preprocessing through a sophisticated classifier, such as the 2D-CNN. This streamlines the detection process, making it more efficient by effectively filtering out irrelevant information while remaining adaptable to various image data sources. The utilization of the CNN architecture is a strategic choice in breast cancer classification, as it excels at extracting critical elements that enhance the visibility of malignancies within breast lumps. Early detection of breast cancer is paramount, allowing for timely intervention and treatment before the disease can progress further.

3.1 Dataset Details

In this research, we employ thermal imagery to develop a 2D CNN model for the binary classification of breast cancer. The dataset used for this study is sourced from the freely available DMR-IR database. Access to this database is conveniently provided through a user-friendly online interface, found at [34]. The thermal images used in this study were captured using an FLIR SC-60 camera with a 640 x 480 pixels resolution. The choice of this camera was motivated by its compatibility with MATLAB, making it a practical option for implementation. To enhance the classification accuracy of the collected thermal images, we apply a series of preprocessing steps, including segmentation and convolutional neural network classification techniques. These steps are essential for effectively categorizing breast cancer cases in the dataset.

3.2 Proposed Methodology

The CNN approach has emerged as the most effective method for diagnosing breast cancer because it can extract global features using kernels. These global

features, encompassing accuracy, efficiency, and sensitivity, have proven invaluable for image classification. In our work, we have devised a custom classifier that leverages ML techniques for feature extraction and binary classification. Our classifier is a fusion of two robust architectures: the ResNet structure, which incorporates batch normalization layers after each convolution layer and employs Maxpooling with a layered approach for analyzing benign and malignant tumors. GoogleNet features include the 2D Convolution Layer (2D-CNN) and the ReLU activation function. Through extensive simulations and evaluations, it becomes evident that the 2D-CNN stands out as the optimal classifier. It excels in leveraging filtration and the ReLU activation function, resulting in a transparent and interpretable categorization of thermograms. As such, it emerges as the most proficient choice for breast cancer diagnosis.

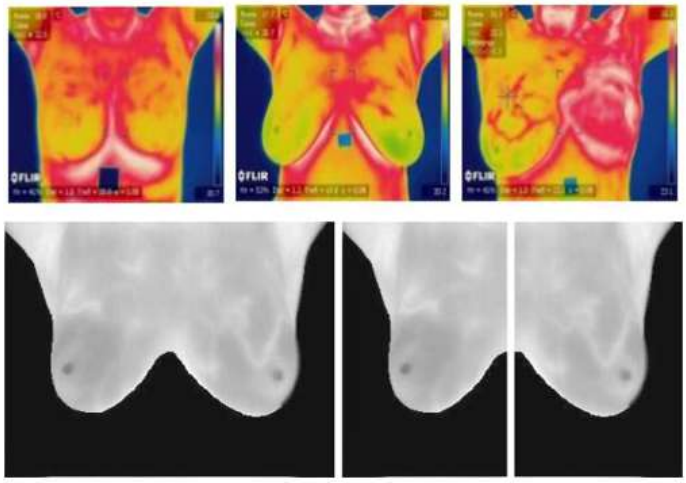

Figure 1. Samples thermograms images from DMR Dataset

- **1*1 Convolution 2D layer** The primary objective of this layer is to minimize the volume of data transmitted across the network, thereby enhancing its depth and breadth. This concept is often called "Network Inside Network," where we employ a 1x1 convolution to analyze the element-wise combination of neighboring pixels in an image. This convolutional operation involves processing the input data alongside a 1x1 filter, resulting in an output with dimensions of 1 x 1. Despite not identifying linear patterns within the image, a 1x1 filter is proficient at capturing commonalities across the image's channels. Consequently, 1x1 convolution filters bring several advantages to the network, aiding in the learning process and serving as a dimensionality reduction technique.
- **1*1 Batch Normalization layer** — Batch normalization is a crucial technique within neural networks, allowing for enhanced independent learning at each layer. It achieves this by normalizing the preceding layers. These normalization processes encompass various aspects, such as scaling the activations of the input layer. Importantly, batch normalization serves a dual purpose: it acts as a potent learning accelerator and a regularization method to prevent overfitting. This layer standardizes the input and outputs, bridging the gap between the convolutional layer and the subsequent activation function (ReLU layer) in the proposed 2D-CNN model.

$$x_{normalized} = x - m \,/\, x_{max} - x_{min}$$

Here 'x' represents several crucial aspects: the maximum value, the minimum value, the mean of the dataset, and the specific data point that is to undergo normalization.

- **1*1 ReLU layer** — A rectifier function, such as Rectified Linear Unit (ReLU), Leaky ReLU, TanH, or Sigmoid, plays a crucial role in refining the output of each kernel operation. Among these options, ReLU stands out as the most efficient choice. The ReLU method transforms values less than or equal to zero to zero, allowing the positive values to pass through, thereby enhancing the overall outcome.

$$\sigma(x) = max(0\,x)$$

- **Max Pooling 2D Layer** — A new layer, referred to as a pooling layer, has been introduced in the network architecture. This pooling layer follows a ReLU layer in the sequence. It employs a specific pooling technique called max pooling, which

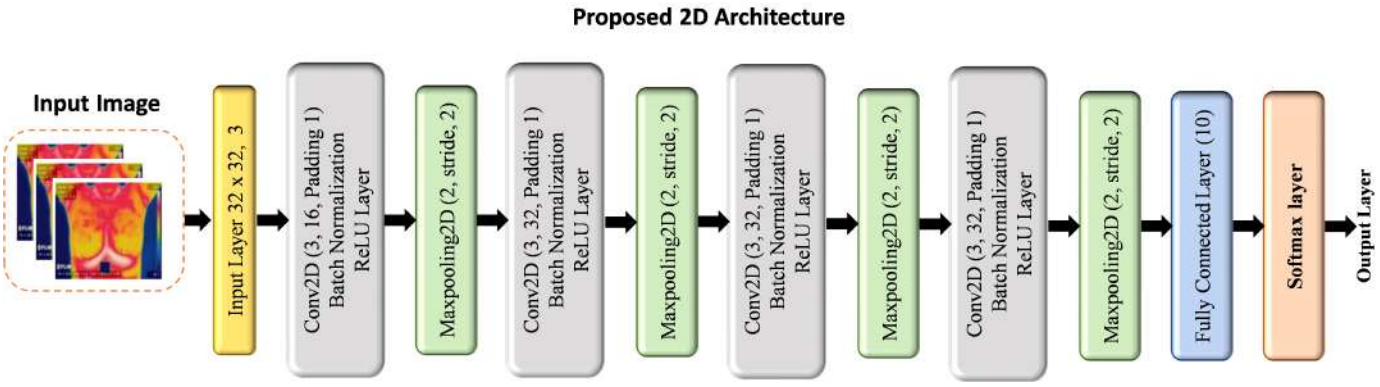

Figure 2. Layered Architecture of Proposed 2D-CNN model

selects the maximum value within a defined region of the feature map covered by a filter. As a result, this operation generates a feature map highlighting the most prominent elements from the previous feature map. During computation, the max-pooling layer considers only the highest values within a specified kernel size. In this case, a 2-by-2 kernel is used to process the entire input image, resulting in an output image that is reduced to a size of four by four. For each block of four values in the output, the max-pooling operation selects the highest value, effectively capturing the most significant features from the input data.

- **1*1 Fully connected layer** — The information collected from the preceding layers is synthesized to categorize a specific image. The initial max pooling layer's output is flattened before its transmission to the Fully Connected layer.
- **Softmax Layer** — The SoftMax function plays a crucial role in deep learning by transforming the output of a fully connected layer into a probability distribution ranging from 0 to 1. This probability distribution is essential for classifying data. It's important to note that this layer incorporates normalized exponential functions. In a fully connected layer's topmost tier, every neuron establishes full connectivity with the preceding fully connected layer, resembling the connectivity pattern found in conventional neural networks.

$$f_j^l = \sigma \sum_{i=1}^{N^{l-1}} * k_{ij} b_j^l$$

The layer before the Soft-Max Layer is identified as follows:

$$h_p^{end} = \omega^{end} * h_p^{end-1} + b^{end}$$

The normalized outcome using the Soft-Max regression is as follows:

$$\bar{y}_p = -exp(h_p^{end}) \backslash \sum_{p=1}^{2} exp(h_p^{end})$$

- **Classification Output Layer** — The design phase has been successfully concluded. During this phase, every input is categorized into one of the exclusive classes within this layer based on the probabilities calculated by the softmax layer for each information. After training completion, the trained network is applied to categorize the validation set. Our 2D-CNN model achieved a remarkable 95% success rate in this endeavor.
- **Hidden Layer** — To build a deep neural network, it is possible to incorporate multiple hidden layers into the network architecture. In our proposed 2D-CNN model, we have introduced three hidden layers. Notably, each subsequent layer in one batch connects with the last layer in the previous batch. The proposed model is designed with a structural configuration consisting of 27

layers. It operates on images of 32 x 32 pixels and includes five convolution layers, crucial for feature extraction in image data. Additionally, five pooling layers are used to downsample the feature maps, and five normalization layers are used to ensure stable training. The model incorporates the ReLU activation function in all 5 of its layers. Furthermore, there are three fully connected layers towards the end, followed by layers dedicated to rearranging the data and conducting classification using the softmax function. This architecture is well-suited for image processing tasks, with its thoughtful combination of convolutional, pooling, and fully connected layers to effectively learn and represent features in the input data for accurate classification.

4 Experiments and Results

A comprehensive evaluation of the model's performance involves the calculation of various key metrics, including accuracy, specificity, sensitivity, recall, precision, and F-score. These metrics are crucial for conducting a thorough performance analysis. To derive these metrics, we employ a confusion matrix that provides essential information about true positives (TP), false negatives (FN), false positives (FP), and true negatives (TN). True Positives (TP) occur when the 2D-CNN accurately identifies patients as unhealthy. True Negatives (TN) represent cases where the 2D-CNN correctly identifies patients as healthy. False Positives (FP) are instances where the model mistakenly labels a healthy patient as unwell. Conversely, False Negatives (FN) occur when the 2D-CNN incorrectly categorizes a patient as healthy when they are, in fact, unhealthy. This comprehensive evaluation approach ensures a robust assessment of the model's performance across various dimensions.

$$Accuracy = \frac{TP + TN}{TP + FP + TN + FN} \quad (1)$$

$$Precision = \frac{TP}{TP + FP} \quad (2)$$

$$Recall = \frac{TP}{TP + FN} \quad (3)$$

$$F1Score = 2x \frac{Precision \ x \ Recall}{Precision + Recall} \quad (4)$$

4.1 Dataset Distribution

This study utilizes thermal imagery to introduce a 2D CNN model for binary breast cancer classification. The dataset used in this research is from the renowned open-access DMR-IR database [34]. Table presents the dataset distribution.

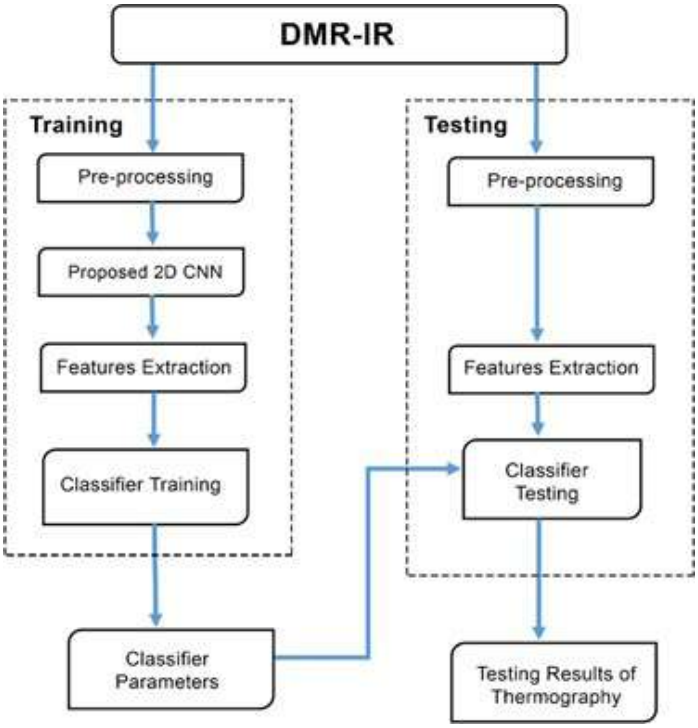

Figure 3. Database Description

Table 1. Dataset Distribution

Dataset	Dimensions	Training	Testing	Total
Batch 1	640 x 480	80%	20%	100
Batch 2	640 x 480	80%	20%	500
Batch 3	640 x 480	80%	20%	4000

In Batch 1, we allocate twenty percent of the dataset for testing. Table 3 presents a comparison of accuracy scores. This table illustrates the results achieved through our proposed approach, 2D-CNN, alongside traditional techniques such as CNN and SVM. Our suggested model capitalizes on enhanced image detection and efficient layering to boost accuracy significantly.

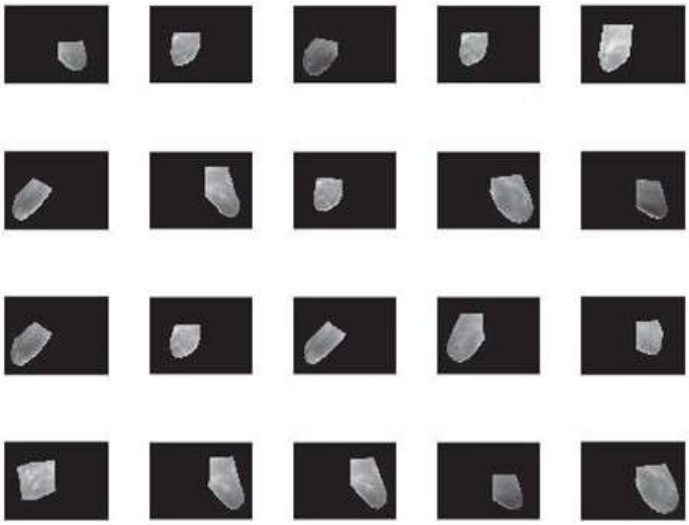

Figure 4. Sample segmented Grey-scale images from dataset

Table 2. Proposed 2D-CNN, CNN, and SVM accuracy with batch 1

Samples	2D-CNN	CNN	SVM
1	82	11	46.5
2	90	96	93
3	13	1	7
4	89	76	82.5
5	61	79	70
6	10	83	46.5
7	27	8	17.5
8	51	38	44.5
9	97	24	60.5
10	88	73	80.5
11	15	39	27
12	87	82	84.5
13	85	17	51
14	43	23	33
15	69	13	41
16	98	12	55
17	36	74	55
18	77	49	63
19	65	46	55.5
20	78	85	81.5
Accuracy	95%	77%	91%

In Batch 2, twenty percent of the dataset is allocated for testing. The comparison of accuracy results is presented in Table 3. This table showcases the outcomes achieved through the suggested 2D-CNN approach, in contrast to conventional techniques such as CNN and SVM. Essentially, our recommended model leverages enhanced image detection capabilities and optimized layering to boost accuracy significantly. Certainly! To ensure that the table fits within the available width while adjusting the width of each column, you can use the pwidth column specifier, where width is the desired width for that column. Here's an example:

Table 3. Proposed 2D-CNN, CNN, and SVM accuracy with batch 2

Samples	2D-CNN	CNN	SVM	Samples	2D-CNN	CNN	SVM
1	408	426	417	51	125	66	95.5
2	452	280	366	52	306	85	195.5
3	64	463	263.5	53	294	20	157
4	454	347	400.5	54	73	284	178.5
5	314	290	302	55	54	126	90
6	49	404	226.5	56	222	240	231
7	138	435	286.5	57	427	309	368
8	270	488	379	58	151	222	186.5
9	472	1	236.5	59	259	237	248
10	474	425	449.5	60	99	197	148
11	78	301	189.5	61	331	55	193
12	475	485	480	62	112	216	164
13	468	258	363	63	445	374	409.5
14	237	234	235.5	64	449	382	415.5
15	389	390	389.5	65	486	478	482
16	69	111	90	66	418	91	254.5
17	205	242	223.5	67	238	246	242
18	443	436	439.5	68	61	278	169.5
19	382	277	329.5	69	65	181	123
20	462	407	434.5	70	111	89	100
21	315	355	335	71	362	408	385
22	18	281	149.5	72	110	36	73
23	406	118	262	73	349	46	197.5
24	446	318	382	74	104	61	82.5
25	324	40	182	75	396	71	233.5
26	360	298	329	76	149	264	206.5
27	353	314	333.5	77	84	244	164

28	186	346	266	78	107	455	281
29	310	421	365.5	79	260	393	326.5
30	81	498	289.5	80	200	307	253.5
31	332	362	347	81	148	310	229
32	15	273	144	82	428	27	227.5
33	130	494	312	83	245	360	302.5
34	22	271	146.5	84	230	486	358
35	46	8	27	85	482	410	446
36	383	57	220	86	119	357	238
37	323	401	362	87	496	326	411
38	147	225	186	88	312	213	262.5
39	440	391	415.5	89	157	74	115.5
40	16	97	56.5	90	234	164	199
41	202	255	228.5	91	32	440	236
42	176	496	336	92	23	13	18
43	351	15	183	93	217	384	300.5
44	364	479	421.5	94	318	123	220.5
45	86	166	126	95	380	120	250
46	223	23	123	96	53	135	94
47	203	223	213	97	417	189	303
48	293	88	190.5	98	190	262	226
49	321	56	188.5	99	5	11	8
50	341	93	217	100	136	338	237

Table 4 presents a comparison of F-scores. This table illustrates the proportion of results achieved through our recommended approach, 2D-CNN, and traditional techniques such as CNN and SVM. Our proposed model capitalizes on enhanced image detection and optimized layering to significantly boost accuracy.

The accuracy results for the 20% dataset are presented in Figure 5. The graph lines exhibit some roughness due to the limited number of images and the maximum number of training samples. As the number of images increases, the graph naturally becomes smoother.

Table 4. Proposed 2D-CNN, CNN, and SVM accuracy with batch 1

Samples	2D-CNN	CNN	SVM
1	0.18	0.1	0.87
2	0.89	0.04	0.99
3	0.53	0.07	0.93
4	0.18	0.1	0.87
5	0.89	0.04	0.99
6	0.53	0.07	0.93
7	0.18	0.1	0.87
8	0.89	0.04	0.99
9	0.53	0.07	0.93
10	0.18	0.1	0.87
11	0.89	0.04	0.99
12	0.53	0.07	0.93
13	0.18	0.1	0.87
14	0.89	0.04	0.99
15	0.53	0.07	0.93
16	0.18	0.1	0.87
17	0.89	0.04	0.99
18	0.53	0.07	0.93
19	0.18	0.1	0.87
20	0.89	0.04	0.99
Accuracy	95%	77%	91%

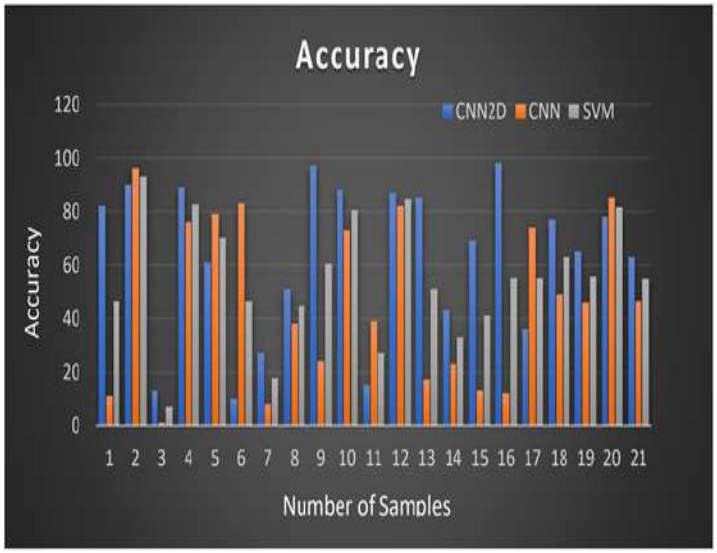

Figure 5. Accuracy results with batch 1

In Figure 6, we display the accuracy results for batch

2. Here, the graph lines also show some roughness, attributed to the high number of training samples and the limited number of images. Like the previous case, the graph becomes smoother as the number of images increases.

Figure 7 illustrates the most favorable accuracy results achieved at epoch 10 using batch size 3. This outcome hints at the underlying factors responsible for the unevenness in the graph lines, specifically, the combination of a limited number of training samples and a small image dataset. We observed a noticeable enhancement in the graph's smoothness as images increased. A similar pattern emerges in Figure 8, showcasing the best accuracy results for batch 3 at epoch 5. However, when examining Figures 9 and 10, we encounter erroneous outcomes for batch 3 at epochs 5 and 10. These results raise concerns about an escalating false rate, seemingly associated with an expanded dataset of images. Interestingly, despite these anomalies, we still observe a natural improvement in graph smoothness as the number of images in the dataset grows.

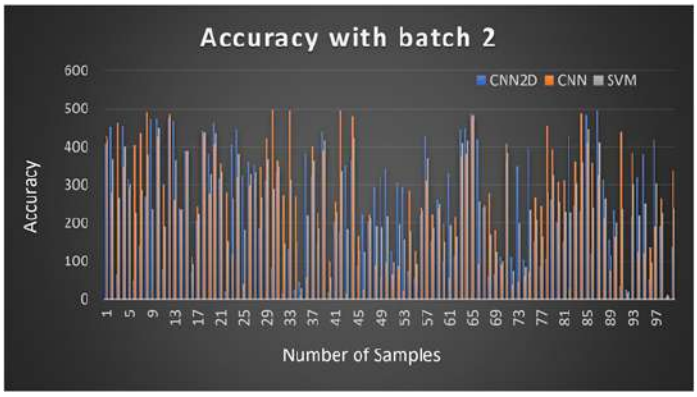

Figure 6. Accuracy results with batch 2

In Figure 11, we present the F-score measurements for 20 separate epochs. The CNN model exhibits a 46% increase in false negatives, which is less desirable for F-score performance. This increase can be attributed to the model's need for more time to detect an image, especially when compared to other models, given a large training dataset. Consequently, this factor significantly impacts the overall detection time.

Similarly, the SVM model demonstrates a 33% increase in the false-negative rate, indicating suboptimal F-score performance. However, the proposed technique stands out by yielding more effective results in terms of F-score performance.

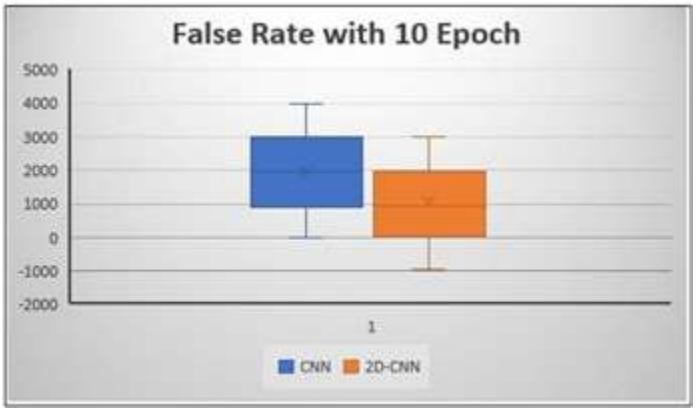

Figure 7. Accuracy results of epoch 10 with batch 3

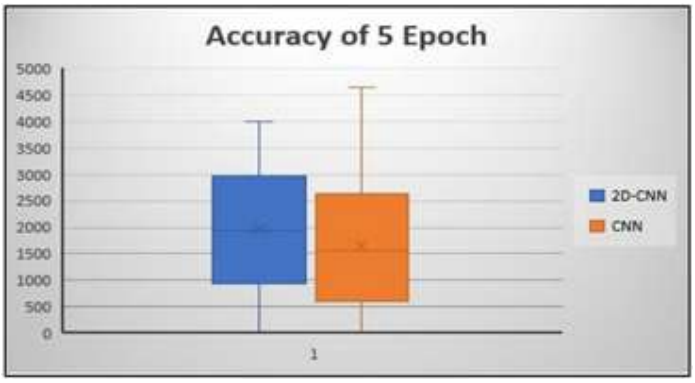

Figure 8. Accuracy results of epoch 5 with batch 3

Table 5 shows various methods and their respective accuracies in a specific domain. Mammoottil et al.'s method, based on Deep Learning (DL), achieved an accuracy of 93.80%. Zuluaga-Gomez et al. utilized CNNs to attain an accuracy of 92.00%. Karthiga et al. employed Support Vector Machines (SVM) and achieved an accuracy of 93.30%. Hakim et al. combined Principal Component Analysis (PCA) with SVM, resulting in an accuracy of 94.40%. However, the proposed model, a customized 2D CNN, outperformed all other methods with an impressive accuracy of 95.01%, demonstrating its superiority in the task.

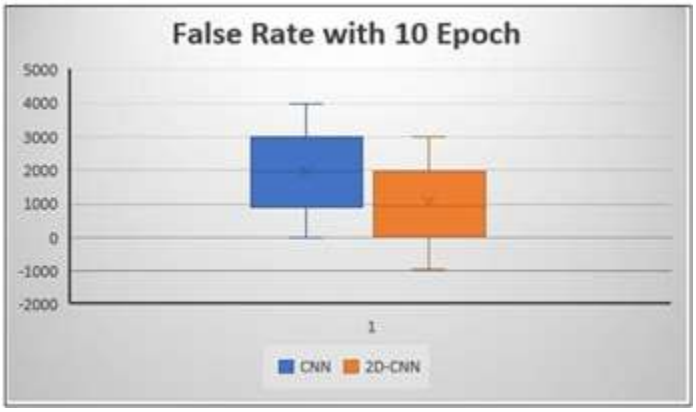

Figure 9. False results of epoch 10 with batch 3

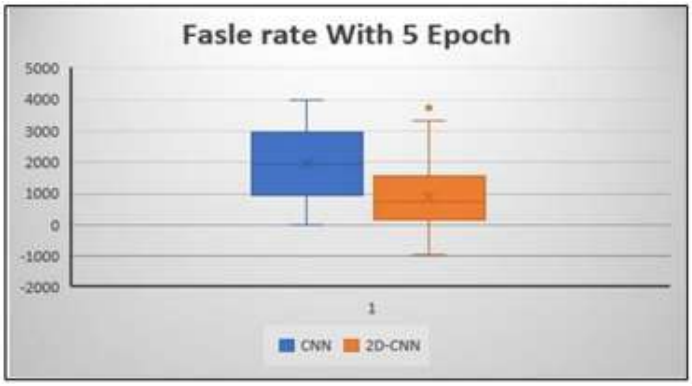

Figure 10. False results of epoch 5 with batch 3

Table 5. Performance Comparison with existing studies

Reference	Method	Accuracy
Mammoottil et al [32]	DL	93.80%
Zuluaga-Gomez et al [33]	CNNs	92.00%
Karthiga et al [31]	SVM	93.30%
Hakim et al [30]	PCA-SVM	94.40%

5 Conclusion

There are various methods for cancer detection, including mammography, ultrasound, and biopsy. However, these methods have drawbacks, such as radiation exposure and uncomfortable procedures. Thermal imaging is a promising alternative for more accurate and less invasive cancer prediction without direct body exposure. In contrast to traditional CNN models, our proposed method demonstrates enhanced results by leveraging a 2D CNN layering technique with three optimized hidden layers. This approach significantly improves classification outcomes on a thermal image dataset. Our method has been fully implemented using MATLAB. It utilizes a segmented dataset comprising thousands of images representing various breast cancer states, although we have focused on a subset of 600 images. Remarkably, our model achieves outstanding results even with a smaller dataset than existing methodologies. For instance, our model achieves a remarkable 95% accuracy rate and an impressive f-score of 0.94 in binary classification between benign and cancerous images. In contrast, traditional models like SVM and standard CNNs achieve lower accuracy rates of 91% and 71%, respectively, on the same dataset. The f-scores for CNN and SVM are also 0.68 and 0.89, respectively. Combining our methodology with other approaches can lead to the creation of a superior model, resulting in improved outcomes in the field of medical image categorization. As layering plays a crucial role in feature detection, our method emphasizes precision and reliability by incorporating precise ranking intensity values into the layering process. This innovative layering combination enhances the overall reliability of our CNN model.

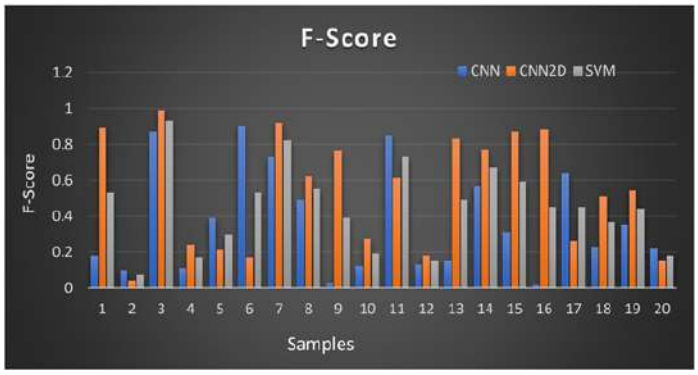

Figure 11. F-score results

Author Contributions

Saif Khan: Conceptualization, Methodology, Data curation, Writing- Original draft preparation , Visualization, Investigation **Asif**: Data curation, Writing- Original draft preparation. **Tanveer Meeran & Umair Bilhaj**: Visualization, Investigation.

Compliance with Ethical Standards

It is declare that all authors don't have any conflict of interest. It is also declare that this article does not contain any studies with human participants or animals performed by any of the authors. Furthermore, informed consent was obtained from all individual participants included in the study.

Funding Information

No Funding

References

[1] American cancer society.about breast cancer.org—1.800.227.2345. *WHO* 2020.

[2] N. Dey, A. S. Ashour, and A. S. Althoupety, "Thermal imaging in medical science," in emphRecent Advances in Applied Thermal Imaging for Industrial Applications, 2017, pp. 87-117.

[3] E. Daniela and M. Reynoso, "Diagnosis of breast cancer through the emphprocessing of thermographic images and neural networks," 2017.

[4] M. Waqas, M. A. Tahir, and R. Qureshi, "Ensemble-based instance relevance estimation in multiple-instance learning," emphin 2021 9th European Workshop on Visual Information Processing (EUVIP), 2021, pp. 1-6.

[5] M. Waqas, M. A. Tahir, and R. Qureshi, "Deep Gaussian mixture model based instance relevance estimation for multiple instance learning applications," emphApplied intelligence, vol. 53, no. 9, pp. 10310-10325, 2023.

[6] M. Waqas, M. A. Tahir, and S. A. Khan, "Robust bag classification approach for multi-instance learning via subspace fuzzy clustering," emphExpert Systems with Applications, vol. 214, p. 119113, 2023.

[7] S. T. Kakileti et al., "Personalized risk prediction for breast cancer pre-screening using artificial intelligence and thermal radiomics," emphArtificial Intelligence in Medicine, vol. 105, p. 101854, 2020.

[8] M. Hanif, M. Waqas, A. Muneer, A. Alwadain, M. A. Tahir, and M. Rafi, "DeepSDC: Deep Ensemble Learner for the Classification of Social-Media Flooding Events," emph-Sustainability, vol. 15, no. 7, p. 6049, 2023.

[9] R. Roslidar, A. Rahman, R. Muharar, M. R. Syahputra, F. Arnia, M. Syukri, et al., "A review on recent progress in thermal imaging and deep learning approaches for breast cancer detection," emphIEEE Access, vol. 8, pp. 116176-116194, 2020.

[10] S. Ansari and S. Salankar, "An Overview on Thermal Image Processing," emphin Proc. Second Int. Conf. Res. Intell. Comput. Eng., 2017, vol. 10, pp. 117–120.

[11] A. Akula, R. Ghosh, and H. K. Sardana, "Thermal imaging and its application in defence systems," emphAIP Conf. Proc., vol. 1391, pp. 333–335, 2011, doi: 10.1063/1.3643540.

[12] R. Vardasca, L. Vaz, and J. Mendes, "Classification and decision making of medical infrared thermal images," emphin Lect. Notes Comput. Vis. Biomech., 2018, vol. 26, pp. 79–104.

[13] B. B. Lahiri, S. Bagavathiappan, T. Jayakumar, and J. Philip, "Since January 2020 Elsevier has created a COVID-19 resource centre with free information in English and Mandarin on the novel coronavirus COVID- 19 . The COVID-19 resource centre is hosted on Elsevier Connect , emphthe company ' s public news and information ," no. January, 2020.

[14] A. Duarte et al., "Segmentation Algorithms for Thermal Images," emphProcedia Technol., vol. 16, pp. 1560–1569, 2014, doi: 10.1016/j.protcy.2014.10.178.

[15] D. Singh and A. K. Singh, "Role of image thermography in early breast cancer detection- Past, present and future," emphComput. Methods Programs Biomed., vol. 183, 2020, doi: 10.1016/j.cmpb.2019.105074.

[16] R. Resmini, A. Conci, U. Federalfluminense, A. Silva, E. Diniz, and U. F. Fluminense, "THERMAL FEATURE ANALYSIS TO AID ON BREAST DISEASE," no. March 2016, 2011.

[17] M. A. Farooq and P. Corcoran, "Infrared Imaging for Human Thermography and Breast Tumor Classification using Thermal Images," emphin 2020 31st Irish Signals Syst. Conf. ISSC 2020, 2020, doi: 10.1109/ISSC49989.2020.9180164.

[18] A. Al Nahid and Y. Kong, "Involvement of Machine Learning for Breast Cancer Image Classification: A Survey," emphComput. Math. Methods Med., vol. 2017, no. i, 2017, doi: 10.1155/2017/3781951.

[19] F. Alfayez, M. W. A. El-soud, and T. Gaber, "Thermogram Breast Cancer Detection : A Comparative Study of Two Machine Learning Techniques," 2020, doi: 10.3390/app10020551.

[20] M. A. S. Al Husaini, M. H. Habaebi, T. S. Gunawan, M. R. Islam, and S. A. Hameed, "Automatic Breast Cancer Detection Using Inception V3 in Thermography," pp. 255–258, 2021, doi: 10.1109/iccce50029.2021.9467231.

[21] P. S. Pawar and D. R. Patil, "Breast cancer detection using neural network models," in Proc.- 2013 Int. Conf. Commun. emphSyst. Netw. Technol. CSNT 2013, 2013, pp. 568–572.

[22] I. Dabral, M. Singh, and K. Kumar, "Cancer Detection Using Convolutional Neural Network," in Lect. emphNotes Networks Syst., 2021, vol. 175, pp. 290–298.

[23] J. Zuluaga-Gomez, Z. Al Masry, K. Benaggoune, S. Meraghni, and N. Zerhouni, "A CNN- based methodology for breast cancer diagnosis using thermal images," emph-Comput. Methods Biomech. Biomed. Eng. Imaging Vis., vol. 9, no.

[24] J. C. Torres-Galván, E. Guevara, and F. J. González, "Comparison of Deep Learning Architectures For Pre-Screening of Breast Cancer Thermograms," emph2018 IEEE International Symposium on Computer Applications & Industrial Electronics (ISCAIE), pp. 2–3, 2019. doi: 10.1109/PN.2019.8819587.

[25] S. J. Mambou, P. Maresova, O. Krejcar, A. Selamat, and K. Kuca, "Breast cancer detection using infrared thermal imaging and a deep learning model," emph-Sensors (Switzerland), vol. 18, no. 9, Sep. 2018. doi: 10.3390/s18092799.

[26] G. J. Zuluaga, Z. Al Masry, K. Benaggoune, S. Meraghni, and N. Zerhouni, "A CNN-based methodology for breast cancer diagnosis using thermal images," emphComput Methods Biomech Biomed Eng Imaging Vis, 2020. doi: 10.1080/21681163.2020.1824685.

[27] G. I. Sayed, M. Soliman, and A. E. Hassanien, "Bio-inspired swarm techniques for thermogram breast cancer detection," in Medical Imaging in Clinical Applications: Algorithmic and Computer-Based Approaches, pp. 487–506, emphSpringer International Publishing, 2016.

[28] A. Hakim and R. N. Awale, "Harnessing the power of machine learning for breast anomaly prediction using thermograms," emphInternational Journal of Medical Engineering and Informatics, vol. 15, no. 1, pp. 1-22, 2023.

[29] R. Karthiga and K. Narasimhan, "Medical imaging technique using curvelet transform and machine learning for the automated diagnosis of breast cancer from thermal image," emphPattern Analysis and Applications, vol. 24, no. 3, pp. 981-991, 2021.

[30] M. J. Mammoottil, L. J. Kulangara, A. S. Cherian, P. Mohandas, K. Hasikin, and M. Mahmud, "Detection of breast cancer from five-view thermal images using convolutional neural networks," emphJournal of Healthcare Engineering, 2022.

[31] J. Zuluaga-Gomez, Z. Al Masry, K. Benaggoune, S. Meraghni, and N. Zerhouni, "A CNN-based methodology for breast cancer diagnosis using thermal images," emphComputer Methods in Biomechanics and Biomedical Engineering: Imaging & Visualization, vol. 9, no. 2, pp. 131-145, 2021.

[32] S. U. R. Khan, M. Zhao, S. Asif, X. Chen, and Y. Zhu, "GLNET: global–local CNN's-based informed model for detection of breast cancer categories from histopathological slides," emphThe Journal of Supercomputing, 2023. doi: [DOI to be added when available].

[33] S. U. R. Khan, M. Zhao, S. Asif, and X. Chen, "Hybrid-NET: A fusion of DenseNet169 and advanced machine learning classifiers for enhanced brain tumor diagnosis," emphInternational Journal of Imaging Systems and Technology, doi: 10.1002/ima.22975.

[34] S. Chatterjee, S. Biswas, A. Majee, S. Sen, D. Oliva, and R. Sarkar, "Breast cancer detection from thermal images using a Grunwald-Letnikov-aided Dragonfly algorithm-based deep feature selection method," emphComputers in Biology and Medicine, vol. 141, 105027, 2022.